

Modelling of deep adsorptive desulphurization of methanol for fuel cell applications

Eugeniusz Molga* , Robert Cherbański , Andrzej Stankiewicz , Michał Lewak 

Warsaw University of Technology, Chemical and Process Engineering Department, Waryńskiego 1, 00-645 Warszawa, Poland

Abstract

These studies were carried out within the framework of the European FuelSOME Project (No. 101069828), which focuses on establishing a multi-fuel energy generation system based on utilization of Solid Oxide Fuel Cells (SOFC) and is dedicated mainly to the long-distance maritime shipping. For the SOFC stacks, the removal of sulphur contaminations from fuels is crucial as the content of sulphur compounds is strictly limited, even to dozens of mol ppb.

The modelling and calculations were performed for a selected testing system of deep adsorptive purification of methanol to remove dibenzothiophene (DBT) on activated carbon (AC), where DBT was taken as a representative of sulphur compounds contaminating methanol. An appropriate model of the adsorption column packed with activated carbon pellets was elaborated as a basis for process simulations and further techno-economic considerations. The research focused on modelling sulphur removal to achieve the required purity of methanol, then on cost analysis to optimize the proposed purification process. At the current stage, the aim of the performed studies was a preliminary check of a possibility of successfully performing deep adsorptive desulphurisation of methanol and an estimation of purification costs.

Keywords

methanol purification, sulphur removal, adsorber modelling, techno-economic analysis, process optimization

* Corresponding author, e-mail:
eugeniusz.molga@pw.edu.pl

Article info:

Received: 29 April 2024

Revised: 10 August 2024

Accepted: 27 August 2024

1. INTRODUCTION

Shipping is responsible for the annual emission of about 1 billion tons of carbon dioxide (CO₂) and about 2.5% of global anthropogenic greenhouse gas (GHG) emissions worldwide – e.g. see (European Commission, Directorate-General for Climate Action, 2019). Most ocean-going vessels operate using heavy fractions of petroleum, so GHG and air pollutants from ships, such as carbon dioxide (CO₂), nitrogen oxides (NO_x), sulphur oxides (SO_x) and particulate matters (PM), have to become key regulatory targets, in the EU and at a global level. The above issues are addressed, among other things, by the European FuelSOME project (FuelSOME, 2022). This project focuses on establishing the technological feasibility of a flexible, scalable, and multi-fuel capable energy generation system based on utilization of Solid Oxide Fuel Cells (SOFC) technology, specially dedicated to the long-distance maritime shipping.

Since hydrogen use on deep sea vessels is strongly limited due to difficulties of its storage and transportation, it is assumed that the proposed system should be able to operate mainly using ammonia and methanol. Therefore, the main challenge leading to the realization of such concept is to provide sufficient quantity of fuels, which meet strong quality requirements specific for the SOFC system.

Considering methanol as a very promising on-board fuel for fuel cell-powered vehicles and ships, the feedstocks and its production methods should be taken into account and evaluated.

A schematic diagram to summarize methods for production of methanol as a fuel for SOFC applications is shown in Fig. 1, where the non-renewable and renewable pathways are distinguished.

Different aspects of methanol use as an energy carrier are discussed in great detail in a review by Araya et al. (2020), where special attention is paid to renewable production methods.

In the literature of subject plenty of reports on methanol specifications can be found – e.g. see (Marcus and Glinberg, 1985). However, in the current times it is good to rely on regularly updated recommendations of the Methanol Institute (<https://www.methanol.org>), where it is stated that methanol is typically produced to meet the methanol specifications of the International Methanol Producers and Consumers Association (IMPCHA). The current IMPCHA Methanol Reference Specifications, updated in July 2021, can be found on the IMPCHA website (IMPCHA, 2021), where as many as 18 specifications are characterized – i.e. a given physico-chemical property and/or acceptable concentration of any impurity is described quantitatively and also standardized analytical methods to determine this are indicated. These reference specifications are listed in Table 1.

Comparing purity requirements for SOFC application to the indications given by the IMPCHA in Table 1 it should be expected that the majority of methanol on the market does not meet so strong demands. This is because the sulphur content in methanol for SOFC applications is limited by SOFC stack producers to even 30 mol-ppb (Elcogen, 2020), while



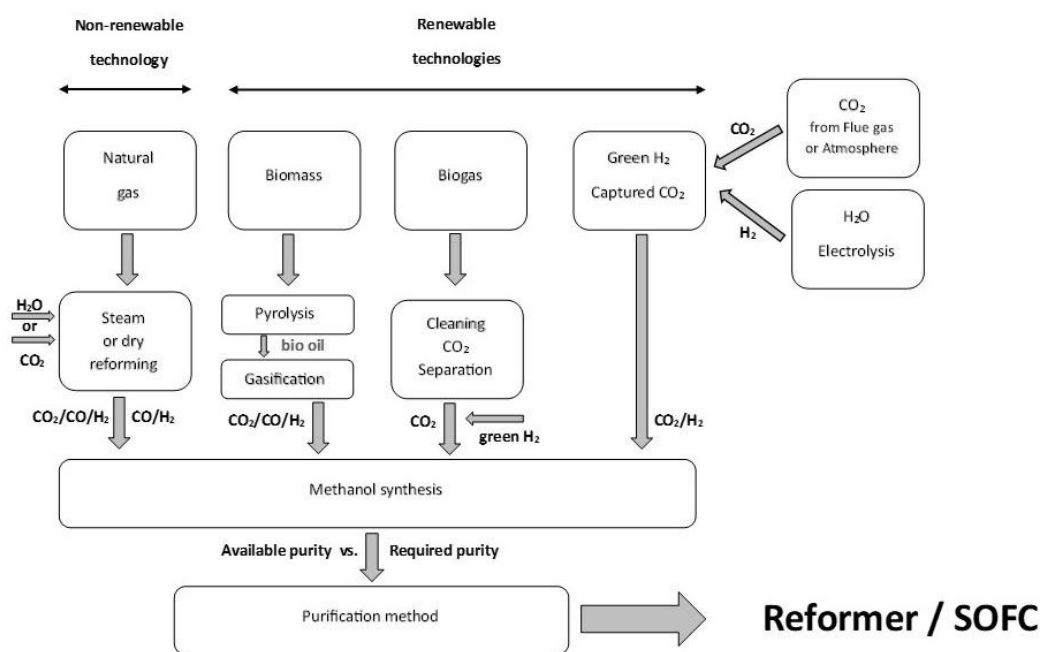


Figure 1. Schematic diagram to illustrate production and utilization of methanol as a fuel for SOFC.

Table 1. Methanol reference specifications recommended by the International Methanol Producers and Consumers Association (IMPCA) – (IMPCA, 2021).

	Test	Unit	Limiting value	Analytical Method
1.	Appearance		Clear and free from suspended matter	IMPCA 003
2.	Purity on dry basis	% w/w	Min 99.85	IMPCA 001
3.	Acetone	mg/kg	Max 30	IMPCA 001
4.	Ethanol	mg/kg	Max 50	IMPCA 001
5.	Colour	Pt–Co	Max 5	ASTM D 1209
6.	Water	% w/w	Max 0.100	ASTM D 5386
7.	Distillation range at 760 mmHg	°C	Max 1.0	ASTM D 1078
8.	Specific gravity 20 °C	–	0.7910–0.7930	ASTM D 4052
9.	Potassium permanganate time test at 15 °C	minutes	Min 60	ASTM D 1363
10.	Chloride as Cl ⁻	mg/kg	Max 0.5	IMPCA 002
11.	Sulphur	mg/kg	Max 0.5	ASTM D 3961 ASTM D 5453
12.	Water miscibility (hydrocarbons)	–	Pass test	ASTM D 1722
13.	Carbonisables	Pt–Co	Max 30	ASTM E 346
14.	Acidity as acetic acid	mg/kg	Max 30	ASTM D 1613
15.	Iron in solution	mg/kg	Max 0.10	ASTM E 394
16.	Non-volatile matter	mg/1000ml	Max 8	ASTM D 1353
17.	TMA	–	TMA test	ASTM E 346
18.	Aromatics	–	UV-scan	IMPCA 004

the limiting sulphur concentrations in methanol recommended by the IMPCA (see Table 1) is equal to 0.5 mg/kg, which is equivalent to 500 mol-ppb. Because of that methanol for SOFC applications should be always carefully analysed and pretreated before using.

The choice of methanol purification method depends on its production technology as well as on used feedstocks. Water is indicated as the main impurity of methanol, so from this point of view and considering that methanol is a good solvent for electrolytes, a content of dissolved salts in methanol becomes an important issue. Generally, electrolytes which are well soluble in water, are with some exceptions also soluble in methanol. The solubilities of some salts of the alkali metals in methanol are shown in Table 2.

Table 2. Molal solubilities in [mol/kg MeOH] of some salts of alkali metals in methanol at 25 °C (Marcus and Glinberg, 1985).

	F ⁻	Cl ⁻	Br ⁻	I ⁻	NO ₃ ⁻	CO ₃ ²⁻	SO ₄ ²⁻
Li ⁺	0.0068	4.95	3.95	*vs	6.23	0.0075	0.0115
Na ⁺	0.0055	0.240	1.56	4.17	0.345	0.0293	0.0008
K ⁺	0.394	0.071	0.175	1.029	0.0376	0.447	3 · 10 ⁻⁵
Rb ⁺		0.111					
Cs ⁺		0.215			0.0121		
*vs – very soluble							

A special question discussed in the literature is whether silica dissolves in methanol. Although this is particularly important for flush column chromatography, it can be also relevant for utilization of methanol as a fuel for SOFCs. The majority of literature sources confirm that silica does dissolve in methanol, although the Biotage reports the opposite (Biotage, 2023).

The purity of purchased methanol is very important but because of subsequent operations – e.g. transportation, storage, and fuelling, a more detailed analysis of the methanol fate on its way from the manufacturer to the fuel cell stacks is necessary. Appropriate analytical methods should be used to effectively estimate the purity of methanol at every stage of that way, but particularly just before feeding to the SOFC stacks. These methods should be rapid, accurate and easy to use.

The simplest way to check methanol purity is to measure its density, which can be used for crude methanol to determine significant amounts of water present. Other methods for the determination of water in methanol depend on its concentration.

For the determination of the residual impurities in methanol (down to ppm levels) gas chromatography is the best for detection of organic impurities, while flameless atomic absorption for heavy metals (Marcus and Glinberg, 1985). However, more complex methods – such as HPLC, HPLC-UV-MS (Spingern et al., 1981) and SPE – solid phase extraction (Poole, 2003) can also be employed.

Regardless of methanol synthesis technology, the post-production treatment is fundamental for obtaining a high purity methanol stream. In industrial and analytical practice methanol purification processes usually include removal of water and organic impurities, production of conductivity-grade solvent and removal of bases and heavy metals.

Distillation, which is an immanent element of methanol production, is widely employed and is extensively described in the literature. Numerous articles and patents dedicated to this topic focus on the effectiveness of purification process as well as the economic analysis, because distillation consumes a significant amount of energy – e.g. see (Fiedler et al., 2002; Luis et al., 2014; Moiola and Pellegrini, 2021; Montevecchi et al., 2024; Pinto, 1980; Rocha et al., 2017; Villegas et al., 2015; Zhang et al., 2010).

In some special cases, e.g. when a specific impurity forms an azeotrope with the methanol, a distillation can be coupled with another separation technique, such as pervaporation (Luis et al., 2014; Villegas et al., 2015) or extraction (Gil et al., 2009; Gracová and Vavrušová, 2018) to effectively improve the removal of that impurity.

Purification by distillation process can be effectively utilized at the methanol production plant for massive streams of methanol and significant amounts of impurities. However, for the removal of residual impurities to meet high purity requirements – e.g. those for fuel cells – more sophisticated methods should be applied. These include adsorptive separation applied either as simple adsorption in a column filled with the sorbent or as continuous simulated moving bed chromatography (Lee et al., 2002; Wen et al., 2010). It should be pointed out that methanol preconditioning by adsorption can be carried out only to reach strong SOFC requirements, so it is reasonably only for removal of trace impurities.

Although, according to our knowledge, there are no publications on deep desulfurization of methanol (including also adsorptive desulfurization), valuable indications for a similar process can be found in a recent review paper by Saha et al. (2021). This paper is devoted to desulphurization of petroleum fuels, although systematized information on adsorbents for sulphur removal, process kinetics and thermodynamics as well as on process parameters help to search for a proper solution also for methanol purification.

Additionally, considering a choice of methanol purification method it should be necessarily considered that in the FuelSOME Project methanol is not directly fed to the SOFC stacks, but it is first decomposed in the reformer. Therefore, methanol contamination by water is not important if its content does not significantly influence the methanol reforming process. However an influence of water present in the methanol on the adsorptive removal of contaminants can be crucial for efficiency of purification process. Also, the presence

of non-volatile inorganic salts, silica and others is not relevant as long as they are not thermally decomposed in the reformer and can be effectively removed from it.

In this paper deep adsorptive removal of sulphur from methanol for SOFC applications is modelled and analysed to check the possibility of successful performance of this process as well as to estimate purification costs.

2. MODELLING OF ADSORPTIVE SULPHUR REMOVAL FROM METHANOL

Purification of methanol by adsorption was investigated for the following testing system: methanol contaminated with dibenzothiophene (DBT) – activated carbon (AC). DBT was taken as a representative of sulphur compounds contaminating methanol, while activated carbon was assumed as the sorbent, since it is very efficient in removal of sulphur compounds (Lee et al., 2002).

Modelling and further considerations were performed for deep adsorptive desulphurization process carried out in a cylindrical column packed with spherical particles of activated carbon.

In general case, the mass balance for DBT adsorption carried out over a differential control volume (i.e. along the differential column length – Δz) consists of two balance equations written for the liquid and solid phase, respectively. These balance equations must take into account and describe all stage processes and phenomena occurring in the considered system – i.e. the convective and dispersive flow of liquid through the column bed, the mass transfer from bulk of liquid to sorbent grains, the diffusional transport in the pores of sorbent as well as the adsorption rate and adsorption equilibrium. All of this results in a quite complex set of model equations and therefore appropriate simplifications are usually sought.

Based on the statistical moment analysis – e.g. see (Carbonell and McCoy, 1975; Molga, 2009; Schneider and Smith, 1968) – a quantitative estimation of significance of each stage process was possible. Using this statistical moment analysis a series of calculations was carried out for process parameters listed in Table 3 and the range of operating parameters indicated in Table 4. However, it should be pointed out that some simplifications were required to utilize this method of moments – e.g. the adsorption equilibrium was approximated with a linear dependence. It was found that a significance of each above mentioned component process depends strongly on the sorbent particle diameter and to a lesser extent on the liquid interstitial velocity. Usually the results obtained with the analysis of statistical moments supply valuable indications for simplification of the full model. However, in the considered case, due to a quite wide range of the considered process operating conditions, a contribution of each stage process changes significantly depending on the considered

case. Therefore, to keep a model description consistent and clear, all stage processes should be taken into account. This can be realized formulating a full model of the considered process, which is given in the Appendix – see Eqs. (A.1–A.11).

Table 3. Model parameters for process carried out at $T = 25^\circ\text{C}$.

Parameter	Value or relationship to calculate	Source
D_L [m ² /s]	$\epsilon Pe_L = 0.20 + 0.011 Re^{0.48}$	Chung and Wen, 1968
k_f [m/s]	$j_D = 1.17 Re^{-0.415}$	Sherwood et al., 1975
D_i [m ² /s]	$2.1 \cdot 10^{-10}$	Carbonell and McCoy, 1975
K_L [m ³ /mol]	0.8036	Wen et al., 2010
q_m [mol/kg]	1.1236	Wen et al., 2010
$k_{1,ad}$ [1/s]	$0.82 \cdot 10^{-3}$	Wen et al., 2010

Kinetic and equilibrium data of Wen (Wen et al., 2010) were here adopted despite the fact that they were determined for the other system, i.e. for the DBT – diesel fuel system, as according to our knowledge no data for the DBT-methanol adsorptive system are available. This was for preliminary estimations only, which have to be verified with the results of our own measurements carried out for the DBT-methanol system.

As the solution of the full model presented in the Appendix (Eqs. A.1–A.11) is a quite complex numerical task, the following simplification was introduced into this model – i.e. the radial distributions of concentrations $c_{DBT,p}$ and q_{DBT} was replaced by the volume average ones: $\overline{c_{DBT,p}}$ and $\overline{q_{DBT}}$, respectively. With this concept the full model of process is significantly simplified, taking simultaneously into account all the mentioned above stage processes.

This simplified version reads now as follows:

- DBT mass balance in the liquid flowing through the packed bed

$$D_L \frac{\partial^2 c_{DBT}}{\partial z^2} - u \frac{\partial c_{DBT}}{\partial z} - \frac{6(1-\epsilon)}{\epsilon d_p} K_{gI} (c_{DBT} - \overline{c_{DBT,p}}) = \frac{\partial c_{DBT}}{\partial t} \quad (1)$$

- DBT mass balance inside the sorbent particle

$$\epsilon_p \frac{\partial \overline{c_{DBT,p}}}{\partial t} = \frac{6}{d_p} K_{gI} (c_{DBT} - \overline{c_{DBT,p}}) - (1 - \epsilon_p) \rho_s \frac{\partial \overline{q_{DBT}}}{\partial t} \quad (2)$$

Table 4. The range of process parameters and operating conditions, for which model calculations were carried out.

Column and bed configuration					Operating conditions		Methanol properties	
L	D_w	ε	ε_p	d_p	G	$c_{\text{DBT},\text{in}}$	ρ_M	μ_M
[m]	[m]	[-]	[-]	[m]	[kg/h]	[mol/m ³]	[kg/m ³]	[Pacots]
5.0	0.1 ÷ 0.5	0.45	0.55	0.001 ÷ 0.010	10 ÷ 500	2.15 ÷ 64.50	792	$0.544 \cdot 10^{-3}$

where K_{gl} is the global mass transfer coefficient representing both, external and internal, mass transfer resistances, which is defined as:

$$\frac{1}{K_{gl}} = \frac{1}{k_f} + \frac{1}{k_i} \quad (3)$$

where k_f – is the external mass transfer coefficient, while k_i is the apparent mass transfer coefficient representing internal mass transfer resistances, which is calculated as:

$$k_i = \frac{10D_i}{d_p} \quad (4)$$

The presented concept and the relationship of Eq. 4 was proposed originally by (Glueckauf, 1955), then repeatedly checked and applied by numerous researchers to describe the adsorption processes carried out in the column – e.g. see (Constantino et al., 2015; Santacesaria et al., 1982; Silva et al., 2011).

The effective intraparticle diffusion coefficient D_i [m²/s], appearing in Eq. 4 is calculated as:

$$D_i = \frac{D_M \varepsilon_p}{\tau} \quad (5)$$

where D_M [m²/s] is the molecular diffusion coefficient for DBT in the methanol, while τ [-] is the tortuosity factor and ε_p – sorbent particle porosity.

The rate of adsorption $\frac{\partial q_{\text{DBT}}}{\partial t}$ appearing in Eq. 2 can be easily estimated assuming adsorption equilibrium, so applying the equilibrium equation of Eq. A.5 it can be expressed in terms of the appropriate volume average concentration in liquid filling pores $\overline{c_{\text{DBT},p}}$.

The set of model equations (Eqs. 1–2) can be solved with the following initial conditions:

$$c_{\text{DBT}}(z, 0) = 0 \quad (6)$$

$$\overline{c_{\text{DBT},p}}(z, 0) = 0 \quad (7)$$

together with the Danckwerts boundary conditions:

$$u_{c_{\text{DBT},\text{in}}} = u_{c_{\text{DBT}}} - D_L \frac{\partial c_{\text{DBT}}}{\partial z} \quad (8)$$

at $z = 0$ and at any time

$$\frac{\partial c_{\text{DBT}}}{\partial z} = 0 \quad \text{at } z = L \text{ and at any time} \quad (9)$$

The appropriate values of model parameters appearing in Eqs. (1–9) – D_L , k_f , D_i , K_L , q_m or the relationships to calculate them are given in Table 3.

Notice that the contamination of methanol (shown in Table 4 as the molar concentration $c_{\text{DBT},\text{in}}$) is often expressed as the mass fraction $x_{\text{DBT},\text{in}}$ [% wt.], which can be easily recalculated to the molar concentration following the relationship:

$$c_{\text{DBT},\text{in}} = \frac{x_{\text{DBT},\text{in}} \rho_M}{100 M_{\text{DBT}}} \left[\frac{\text{mol}}{\text{m}^3} \right] \quad (10)$$

Heat effect due to the adsorption process was here neglected due to a small concentration of adsorbed compound. Therefore the heat balance equation was abandoned and adsorption process was assumed to proceed at the constant ambient temperature.

Based on the elaborated model, a series of simulations was carried out for different column and bed configurations as well as different operating conditions. The aim of these investigations was to estimate how the column configuration – i.e. its length L and diameter D_w , the structure of packed bed – i.e. adsorbent particle diameter d_p , bed porosity ε and particle porosity ε_p , as well as operating conditions – i.e. the methanol mass flowrate G and the inlet concentration of DBT $c_{\text{DBT},\text{in}}$ influence the efficiency of the purification process. The range of process parameters and operating variables used to carry out model simulations are listed in Table 4, where a quite wide variability of them can be observed.

The results of simulations supply the DBT concentration profiles in the liquid flowing in the bed interparticle space $c_{\text{DBT}}(z, t)$ and the average concentration in sorbent pores $\overline{c_{\text{DBT},p}}(z, t)$, so also the average concentration of the adsorbed compound $\overline{q_{\text{DBT}}}(z, t)$. However, from the performance point of view the most important is the concentration c_{DBT} as it directly helps to estimate the process efficiency.

Although quite a long column is indicated in Table 4, it does not mean that so long column is proposed to carry out the considered purification process – it was done only to obtain the results for different column lengths with a single calculation run.

3. RESULTS AND DISCUSSION

The carried out simulations supplied the results to find an influence of operating conditions on the efficiency of purification process, so also to carry out optimization of this process.

Note that according to the specifications supplied by the SOFC stack producer (Elcogen, 2020), the maximum concentration of sulphur compounds in the fuel supplied to fuel cells cannot exceed 30 mol-ppb. This means that the maximum molar concentration of DBT in the methanol stream supplied to the fuel cell cannot be higher than:

$$c_{\text{DBT,adm}} = \frac{n_{\text{DBT}} \rho_M}{n_M M_M} = \frac{30}{10^9} \frac{\rho_M}{M_M} = 0.742 \cdot 10^{-3} \left[\frac{\text{mol}}{\text{m}^3} \right] \quad (11)$$

So, for any case the relation between values the admissible concentration of $c_{\text{DBT,adm}}$ and the inlet DBT concentration $c_{\text{DBT,in}}$ determines purification requirements, so also a necessary efficiency of the considered adsorptive purification process.

The set of model equations was implemented within the MATLAB environment and more than 30 series of simulations were performed for different combinations of the d_p , D_w , G and $c_{\text{DBT,in}}$ values.

Typical examples of the obtained results are shown as 2D diagrams in Fig. 2 and Fig. 3. In these diagrams – for each chosen time moment – the DBT concentration profiles c_{DBT} are displayed as a function of location along the adsorption column. In these figures it is clearly visible that at the fixed axial location in the column after a specific time, called the breakthrough time, a non-zero pollutant concentration in the liquid appears. Simultaneously, the zone where the concentration of pollutant in the liquid phase became equal to the inlet concentration $c_{\text{DBT,in}}$ shifts gradually towards the column outlet – this is because of the saturation of the sorbent with the adsorbed compound.

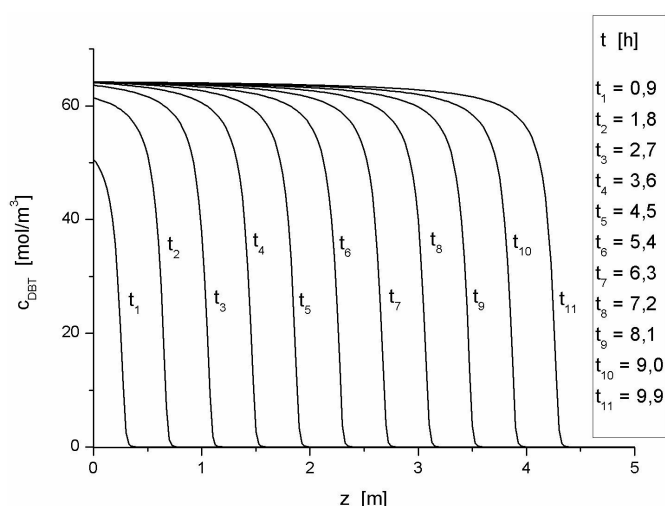


Figure 2. DBT concentrations in the liquid phase c_{DBT} as a function of the location in the adsorbent bed for indicated time moments. Process conditions: $c_{\text{DBT,in}} = 64.2 \text{ [mol/m}^3\text{]}$ (equivalent to the weight percent $x_{\text{DBT,in}} = 1.5\%$), $D_w = 0.3 \text{ [m]}$, $d_p = 0.003 \text{ [m]}$, $G = 500 \text{ [kg/h]}$.

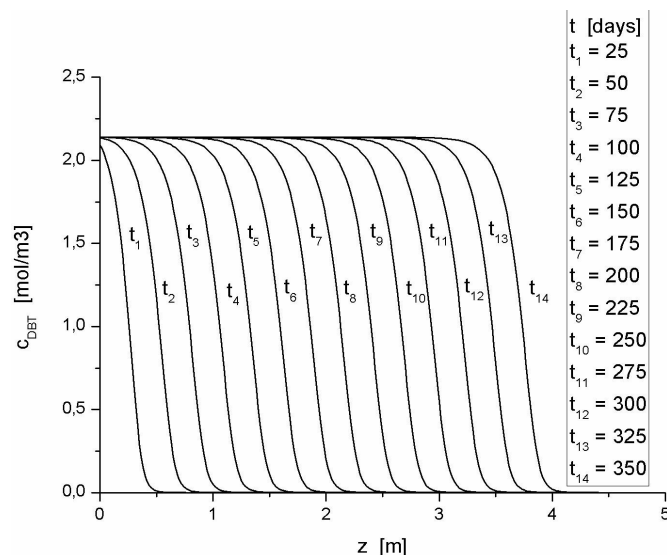


Figure 3. DBT concentrations in the liquid phase c_{DBT} as a function of the location in the adsorbent bed for indicated time moments. Process conditions: $c_{\text{DBT,in}} = 2.14 \text{ [mol/m}^3\text{]}$ (equivalent to the weight percent $x_{\text{DBT,in}} = 0.05\%$), $D_w = 0.3 \text{ [m]}$, $d_p = 0.003 \text{ [m]}$, $G = 10 \text{ [kg/h]}$.

The characteristic feature of the investigated system can be observed in Figs. 2 and 3. Due to a small concentration of pollutant in the purified methanol, the adsorption capacity of sorbent placed in the column is relatively high, so to fully saturate sorbent bed the purification process can be performed for a long time. This time becomes smaller while both, the inlet DBT concentration $c_{\text{DBT,in}}$ and the methanol flow rate G increases. In Figs. 2 and 3 two limiting cases are shown – for the highest considered values of $c_{\text{DBT,in}}$ and G (Fig. 2) the column saturation time is measured in dozens of hours, while for the lowest values of these operating parameters (Fig. 3) the saturation time is as huge as even hundreds of days.

Due to a very high purity demand for methanol used to drive the SOFC stacks, a specific analysis of the considered purification process is proposed taking into account the limiting admissible concentration of sulphur compounds of 30 mol-ppb (equivalent to $0.742 \cdot 10^{-3} \text{ mol/m}^3$).

Such analysis helps to supply data for optimal design of the methanol purification process as well as for its cost evaluation. The proposed methodology is explained in Fig. 4, where the results obtained for any chosen calculation case are schematically shown. For each line, obtained for the time moment t , which describes a dependence of the DBT concentrations in the liquid phase vs. the bed length, the cross-point with the horizontal line indicating the admissible pollutant concentration ($c_{\text{DBT,adm}}$) can be found. This cross-point determines the breakthrough time – t_{Bi} (i.e. the time moment for which the DBT concentration in methanol reaches the admissible value) and the corresponding bed length – L_i . Both values (t_{Bi} and L_i) are crucial for assessment of the purification process performance. At chosen operating conditions for which the

modelling was carried out, the fixed residence time – t_{Bi} (time of the column performance) sets the minimum bed length – L_i necessary to obtain the required methanol purity. However, a different approach can be also applied, when for the fixed column length – L_i the maximum necessary operating time – t_{Bi} can be found. In this case for times $t < t_{Bi}$ the outlet stream of methanol meets the purity requirements, while for times $t > t_{Bi}$ concentration of the pollutant in the outlet stream exceeds this limiting value.

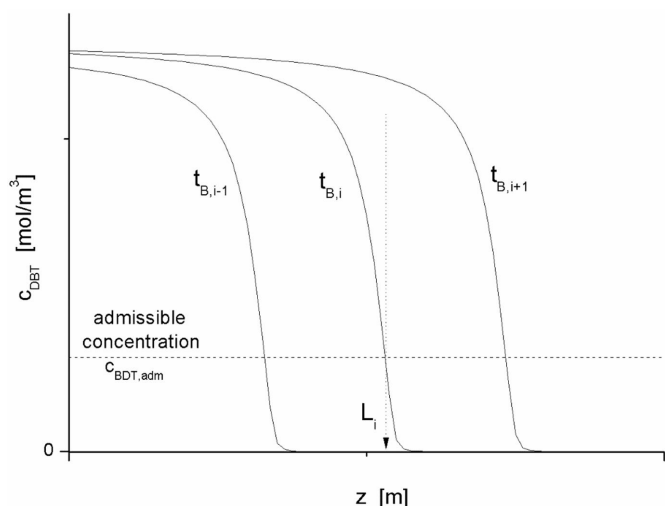


Figure 4. Determination of the dependence between the breakthrough time – t_{Bi} and the corresponding bed length – L_i .

The described procedure was applied for all results obtained from simulations. The process efficiency factor E was introduced to present the results in a form suitable for designing the purification process. This factor is defined as the ratio of mass of the obtained purified methanol to the used sorbent mass as:

$$E = \frac{m_{PM}}{m_A} = \frac{t_{B,i} G}{F_o L_i (1 - \varepsilon) \rho_S} \quad (12)$$

where m_{PM} – is the mass of purified methanol obtained in a single purification run (from the beginning of the process till its stop after time $t_{B,i}$), m_A – mass of sorbent in the column, while $F_o = \pi D_w^2 / 4$ is the cross section area of the empty adsorption column.

Maximizing the value of factor E , the optimal operating conditions for the purification process can be found. In Fig. 5 an operating diagram for optimization the methanol purification is presented, where a significant influence of the methanol mass flow rate G is clearly visible. An increase of the flow rate distinctly deteriorates the process efficiency.

From Fig. 5 it is also visible that the factor E increases with increase of the column length – z , although the influence of the column length on total efficiency of purification process is more complex as the pressure drop in the bed, so also pumping costs, significantly depend on the adsorbent bed length. Because of this, the entire cost analysis should be carried out,

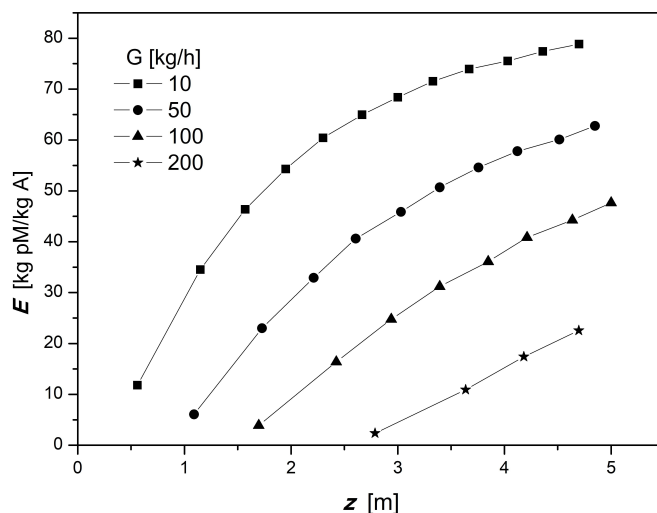


Figure 5. Operating diagram to optimize methanol purification process – dependence of the efficiency factor E vs. the methanol mass flowrate G and the column length z . Process conditions – $c_{DBT,in} = 2.14$ [mol/m³] (equivalent to the weight mass fraction $x_{DBT,in} = 0.05\%$), $D_w = 0.03$ [m], $d_p = 0.003$ [m].

which in a general case should contain the investment cost – C_I , as well as the operating cost – C_O .

The investment costs consist of the permanent part – C_{IP} , which for any considered type of processing facility is almost constant as weakly depends on its size and configuration. The variable part of costs – C_{IV} , significantly depends on the chosen configuration of purification plant. In turn, the operating costs – C_O contain here mainly methanol pumping costs – C_{OP} .

The components of costs listed above can be quantified as follows:

$$C_{IV} = \eta_L L_i + \eta_A m_A \quad (13)$$

where η_L [€/m] is the unit investment cost of the adsorption column (cost for construction of the column per 1 m of length), η_A [€/kg] unit cost of 1kg of adsorbent.

$$C_{OP} = \eta_P \frac{\Delta P}{L} L_i Q t_{B,i} \quad (14)$$

where η_P [€/J] is the unit cost of energy consumed for pumping, $\frac{\Delta P}{L}$ [Pa/m] – the specific pressure drop in the adsorption column per unit length, Q [m³/s] – volumetric flow rate of methanol through the adsorbent bed, where $Q = G/\rho_M$. Notice that the pumping costs – C_{OP} estimated with Eq. 14, so also entire cost analysis, refer to a single purification run, which lasts a period of time $t_{B,i}$.

The specific pressure drop in the adsorption column $\frac{\Delta P}{L}$ can be estimated with the Ergun equation:

$$\frac{\Delta p}{L} = 150 \frac{v_o \mu_M (1 - \varepsilon)^2}{d_p^2 \varepsilon^3} + 1.75 \frac{v_o^2 (1 - \varepsilon)}{d_p \varepsilon^3} \quad (15)$$

where $v_o = \frac{4Q}{\pi D_w^2}$ is the superficial velocity of methanol in the adsorption column.

Finally the total cost of the considered methanol purification process, calculated for a single purification run which lasts a period of time $t_{B,i}$, can be estimated as:

$$C_T = a(C_{Ip} + C_{Iv}) t_{B,i} + C_{Op} \quad (16)$$

where a [1/s] is the depreciation rate.

In search for the optimal performance of the considered purification process, the minimum of the following functional dependency should be found:

$$I = \frac{C_T}{m_{pM}} = \frac{c_T}{t_{B,i}G} = f(D_w, d_p, \varepsilon, G, x_{DBT,in}) \quad (17)$$

where I [€/kg] is the cost indicator determining the total cost of methanol purification per unit mass of the purified product.

So, with use of the elaborated methodology, for any chosen column configuration (D_w, d_p, ε) as well as operating conditions ($G, c_{DBT,in}$), the values of this cost indicator – I can be estimated.

The following values of cost parameters were assumed for calculations as a representative for the considered case: $a = 1/5$ [1/years] = $6.34 \cdot 10^{-9}$ [1/s], $\eta_L = 40$ [€/m], $\eta_A = 10$ [€/kg], $\eta_P = 0.4$ [€/kWh] = $0.11 \cdot 10^{-6}$ [€/J]. These values should be treated only as indicative ones used to demonstrate the proposed method as they can change depending on the year and the country.

An example of the proposed optimization procedure is shown in Fig. 6, where values of the indicator I are displayed vs. the methanol mass flowrate G . As is shown in this figure, for any chosen column and packed bed configuration (D_w, L, d_p, ε) and initial content of sulphur in the methanol ($c_{DBT,in}$) the minimum values of the cost indicator I (expressed here in €/per ton of the purified methanol) can be found. For this value of I the optimal methanol mass flow rate G can be determined.

A similar procedure was repeated for different column and bed configurations – i.e. different data sets of D_w, L, d_p, ε . It has been found that an increase of the sorbent particle diameter slightly deteriorates the sorption efficiency, although this effect is not very pronounced for total cost of process as due to lower pressure drop the pumping costs decrease. Notice that the proposed optimization procedure carried out in a multidimensional domain is a rather complex task, which requires advanced computational tools and skills. Because of this, the elaborated procedure can be difficult for practical application – e.g. in a harbour, as for example the initial content of sulphur ($c_{DBT,in}$) may change from batch to batch. Therefore, a smart and easy to use method was developed. This is an expert system utilizing artificial neural networks (artificial intelligence) which employs the results of performed simulations and techno-economic analysis. The idea of this concept and the obtained results are presented elsewhere (Molga et al., 2024).

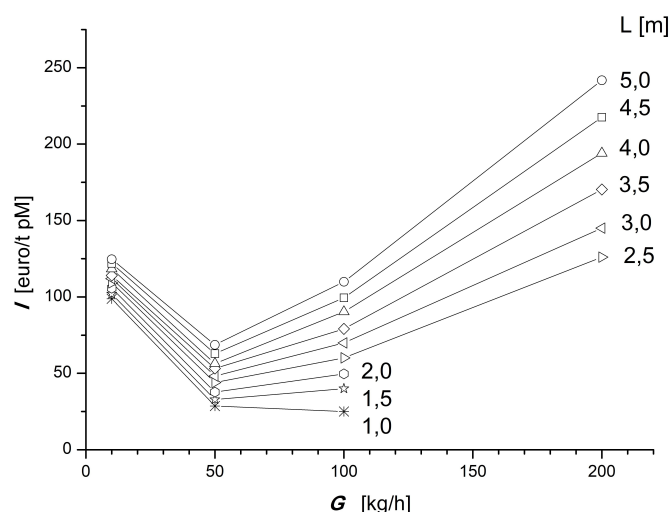


Figure 6. Determination of the optimum operating conditions for methanol purification process. Process conditions – $c_{DBT,in} = 2.14$ [mol/m³] (equivalent to the weight mass fraction $x_{DBT,in} = 0.05\%$), $D_w = 0.03$ [m], $d_p = 0.003$ [m], $\varepsilon = 0.45$.

4. SUMMARY

SOFC systems are very sensitive to the presence of sulphur, so purity requirements for used fuels are very demanding. Typically, the content of sulphur compounds in the fuel-powered SOFC stacks should be not higher than 30 ppb (Elcogen, 2020). According to the specifications indicated for methanol producers by the IMPCA (Table 1) the admissible content of sulphur is much higher than purity requirements defined for the SOFC fuel, therefore an efficient and deep purification of this fuel is necessary. To meet such high purity requirements a deep adsorptive purification method is here recommended and checked. In the performed study, a mathematical model for this purification process was formulated. Based on the results obtained from numerical simulations, the efficiency of the purification process was examined, then the methodology to determine the optimal operating conditions elaborated and presented.

It was found that the application of deep adsorption for methanol purification enables efficient preconditioning of this fuel to meet the very demanding purity requirements.

ACKNOWLEDGEMENTS

This work is a part of the European Union's Horizon Europe research and innovation program "FuelSOME" under Grant Agreement No. 101069828, funded by the European Union. Views and opinions expressed are, however, those of the authors only and do not necessarily reflect those of the European Union. Neither the European Union nor the granting authority can be held responsible for them.

SYMBOLS

a	depreciation rate, 1/year
c_{DBT}	DBT concentrations in the liquid phase in the interparticle space, mol/m ³
$c_{\text{DBT,p}}$	DBT concentrations in the liquid phase in the sorbent pores, mol/m ³
$\overline{c_{\text{DBT,p}}}$	volume average of the local $c_{\text{DBT,p}}$ concentration, mol/m ³
C_{I}	investment cost, €
C_{O}	operating cost, €
C_{Ip}	permanent part of investment cost, €
C_{Iv}	variable part of investment cost, €
C_{OP}	operating costs (pumping cost), €
d_p	adsorbent particle diameter, m
D_i	effective intraparticle diffusion coefficient, m ² /s
D_L	axial dispersion coefficient, m ² /s
D_M	molar diffusion coefficient, m ² /s
D_w	column inner diameter, m
E	process efficiency factor, kg _M /kg _A
G	liquid mass flowrate, kg/h
$I = \frac{C_{\text{T}}}{(t_{\text{B},i}G)}$	cost indicator, €/kg
$j_D = \frac{k_f}{uSc^{0.66}}$	factor for mass transfer, –
$k_{1,\text{ad}}$	adsorption rate constant, 1/s
K_L	constant in the Langmuir equilibrium equation, m ³ /mol
L	column length, m
$Pe = \frac{ud_p}{D_L}$	Peclet number, –
q_{DBT}	concentration of the adsorbed DBT in the solid phase, mol/kg
$\overline{q_{\text{DBT}}}$	volume average of the local $q_{\text{DBT,p}}$ concentration, mol/kg
q_m	constant in the Langmuir equilibrium equation, mol/kg
$Q = G/\rho_M$	liquid volumetric flowrate, m ³ /s
$Re = \frac{u\epsilon d_p}{\nu}$	Reynolds number, –
$Sc = \nu/D_M$	Schmidt number, –
t	time, s
u	liquid interstitial velocity in the bed, m/s
x_{DBT}	mass fraction of pollutant, % wt.
z	axial position, m
$\frac{\Delta P}{L}$	specific pressure drop in the adsorption column, Pa/m
ϵ	bed porosity, –
η_L	unit investment cost of the adsorption column, €/kg
η_A	unit investment cost of the adsorbent, €/kg
η_p	unit cost of energy consumed for pumping, €/J
μ_M	methanol viscosity, Pa·s
ρ_s	density of adsorbent pellets, kg/m ³
ρ_M	methanol density, kg/m ³

Subscripts

adm	admissible
A	adsorbent
B	breakthrough
eq	equilibrium
in	inlet
M	methanol
PM	purified methanol

REFERENCES

- Araya S.S., Liso V., Cui X., Li N., Zhu J., Sahlin S.L., Jensen S.H., Nielsen M.P., Kær S.K., 2020. A review of the methanol economy: the fuel cell route. *Energies*, 13, 596, 1–32. DOI: [10.3390/en13030596](https://doi.org/10.3390/en13030596).
- Biotage, 2023. Does methanol really dissolve silica during flash column chromatography? Available at: <https://www.biotage.com/blog/does-methanol-really-dissolve-silica-during-flash-column-chromatography>.
- Carbonell R.G., McCoy B.J., 1975. Moment theory of chromatographic separation: resolution and optimization. *Chem. Eng. J.*, 9, 115–124. DOI: [10.1016/0300-9467\(75\)80003-7](https://doi.org/10.1016/0300-9467(75)80003-7).
- Chung S.F., Wen C.Y., 1968. Longitudinal dispersion of liquid flowing through fixed and fluidized beds. *AIChE J.*, 14, 857–866. DOI: [10.1002/aic.690140608](https://doi.org/10.1002/aic.690140608).
- Constantino D.S.M., Pereira C.S.M., Faria R.P.V., Loureiro J.M., Rodrigues A.E., 2015. Simulated moving bed reactor for butyl acrylate synthesis: from pilot to industrial scale. *Chem. Eng. Process. Process Intensif.*, 97, 153–168. DOI: [10.1016/j.cep.2015.08.003](https://doi.org/10.1016/j.cep.2015.08.003).
- Elcogen, 2020. *Installation and operation manual of elcoStack® E3000 Version: 1.3*.
- European Commission, Directorate-General for Climate Action, 2019. *Study on methods and considerations for the determination of greenhouse gas emission reduction targets for international shipping – Final report – Technology pathways*. Publications Office. DOI: [10.2834/651129](https://doi.org/10.2834/651129).
- Fiedler E., Grossmann G., Kersebohm D. B., Weiss G., Witte, C., 2002. *Methanol. Ullmann's encyclopedia of industrial chemistry*. Wiley-VCH Verlag/GmbH & Co. DOI: [10.1002/14356007](https://doi.org/10.1002/14356007).
- FuelSOME, 2022. *Multifuel SOFC system with Maritime Energy vectors*. EU Project number 101069828, HORIZON-CL5-2021-D2-01, <https://fuelsome.eu/>.
- Gil I.D., Botía D.C., Ortiz P., Sánchez O.F., 2009. Extractive distillation of acetone/methanol mixture using water as entrainer. *Ind. Eng. Chem. Res.*, 48, 4558–4865. DOI: [10.1021/ie801637h](https://doi.org/10.1021/ie801637h).
- Glueckauf E., 1955. Theory of chromatography. Part 10.– Formulæ for diffusion into sheres and their application to chromathography. *Trans. Faraday Soc.*, 51, 1540–1551. DOI: [10.1039/TF9555101540](https://doi.org/10.1039/TF9555101540).
- Gracová E., Vavrušová M., 2018. Extractive distillation of acetone – methanol mixture using 1-ethyl-3-methylimidazolium trifluoromethanesulfonate. *Chem. Eng. Trans.*, 70, 1190–1194. DOI: [10.3303/CET1870199](https://doi.org/10.3303/CET1870199).

- IMPCA, 2021. *IMPCA methanol reference specifications*. Available at: <https://impca.eu/resources/impca-reference-specifications/>.
- Lee S.H.D., Kumar R., Krumpelt M., 2002. Sulfur removal from diesel fuel-contaminated methanol. *Sep. Purif. Technol.*, 26, 247–258. DOI: [10.1016/S1383-5866\(01\)00174-5](https://doi.org/10.1016/S1383-5866(01)00174-5).
- Luis P., Amelio A., Vreysen S., Calabro V., van der Bruggen B., 2014. Simulation and environmental evaluation of process design: distillation vs. hybrid distillation–pervaporation for methanol/tetrahydrofuran separation. *Appl. Energy*, 113, 565–575. DOI: [10.1016/j.apenergy.2013.06.040](https://doi.org/10.1016/j.apenergy.2013.06.040).
- Marcus, Y. and Glinberg S., 1985. Recommended methods for the purification of solvents and tests for impurities: methanol and ethanol. *Pure Appl. Chem.*, 57, 855–864. DOI: <https://doi.org/10.1351/pac198557060855>.
- Moioli S., Pellegrini L.A., 2021. Study of alternative configurations for methanol purification. *Comput. Aided Chem. Eng.*, 50, 267–272. DOI: [10.1016/B978-0-323-88506-5.50043-7](https://doi.org/10.1016/B978-0-323-88506-5.50043-7).
- Molga E., 2009. *Procesy adsorpcji reaktywnej (Reactive adsorption processes)* (in Polish), WNT, Warszawa, 90–200.
- Molga E., Chwojnowski K., Cherbański R., Stankiewicz A., 2024. Optimization of deep adsorptive purification of methanol for fuel cells – use of expert system based on neural networks application. Book of Abstracts. *XII Polish Scientific Conference, Chemical and Process Engineering for Environment and Medicine*, Sarbinowo, 11–14.09.2024.
- Montecchi G., Cannio M., Cancelli U., Antonelli A., Romagnoli M., 2024. Evaluation of distillery fractions in direct methanol fuel cells and screening of reaction products. *Clean Technol.*, 6, 513–527. DOI: [10.3390/cleantechnol6020027](https://doi.org/10.3390/cleantechnol6020027).
- Pinto A., 1980. *Methanol distillation process*. US Patent US4210495A.
- Poole C.F., 2003. New trends in solid-phase extraction. *TrAC, Trends Anal. Chem.*, 22, 362–373. DOI: [10.1016/S0165-9936\(03\)00605-8](https://doi.org/10.1016/S0165-9936(03)00605-8).
- Rocha L.B., Gimenes M.L., Faria S H.B., Jiménez L., Cavali T., 2017. Design of a new sustainable methanol plant coupled to an ethanol distillery. *Comput. Aided Chem. Eng.*, 40, 805–810. DOI: [10.1016/B978-0-444-63965-3.50136-7](https://doi.org/10.1016/B978-0-444-63965-3.50136-7).
- Saha B., Vedachalam S., Dalai A.K., 2021. Review on recent advances in adsorptive desulfurization. *Fuel Process. Technol.*, 214, 106685, 1–21. DOI: [10.1016/j.fuproc.2020.106685](https://doi.org/10.1016/j.fuproc.2020.106685).
- Santacesaria E., Morbidelli M., Servida A., Storti G., Carra S., 1982. Separation of xylenes on Y zeolites. 2. Breakthrough curves and their interpretation. *Ind. Eng. Chem. Process Des. Dev.*, 21, 446–451. DOI: [10.1021/i200018a017](https://doi.org/10.1021/i200018a017).
- Schneider P., Smith J.M., 1968. Adsorption rate constants from chromatography. *AIChE J.*, 14, 762–771. DOI: [10.1002/aic.690140516](https://doi.org/10.1002/aic.690140516).
- Sherwood T.K., Pigford R.L., Wilke R.L., 1975. *Mass Transfer*. McGraw-Hill, NY, 242.
- Silva V.M.T.M., Pereira C.S.M., Rodrigues A.E., 2011. PermSMBR—a new hybrid technology: application on green solvent and biofuel production. *AIChE J.*, 57, 1840–1851. DOI: [10.1002/aic.12381](https://doi.org/10.1002/aic.12381).
- Spingern N.E., Garvie-Gould C.T., Vuolo L.L., 1981. Analysis of methanol for reversed-phase gradient elution liquid chromatography. *Anal. Chem.*, 53, 565–566. DOI: [10.1021/ac00226a052](https://doi.org/10.1021/ac00226a052).
- Villegas M., Vidaurre E.F.C., Gottifredi J.C., 2015. Sorption and pervaporation of methanol/water mixtures with poly(3-hydroxybutyrate) membranes. *Chem. Eng. Res. Des.*, 94, 254–265. DOI: [10.1016/j.cherd.2014.07.030](https://doi.org/10.1016/j.cherd.2014.07.030).
- Wen J., Han X., Lin H., Zheng Y., Chu W., 2010. A critical study on the adsorption of heterocyclic sulfur and nitrogen compounds by activated carbon: equilibrium, kinetics and thermodynamics. *Chem. Eng. J.*, 164, 29–36. DOI: [10.1016/j.cej.2010.07.068](https://doi.org/10.1016/j.cej.2010.07.068).
- Zhang J., Liang S., Feng X., 2010. A novel multi-effect methanol distillation process. *Chem. Eng. Process. Process Intensif.*, 49, 1031–1037. DOI: [10.1016/j.cep.2010.07.003](https://doi.org/10.1016/j.cep.2010.07.003).

A. APPENDIX

The full model of the considered process of adsorptive purification of methanol consists of the following mass balance equations:

- DBT mass balance in the liquid flowing through the packed bed (in interparticle space)

$$D_L \frac{\partial^2 c_{\text{DBT}}}{\partial z^2} - u \frac{\partial c_{\text{DBT}}}{\partial z} - \frac{6(1-\epsilon)}{\epsilon d_p} N_{\text{DBT}} = \frac{\partial c_{\text{DBT}}}{\partial t} \quad (\text{A.1})$$

where c_{DBT} [mol/m³] is the DBT concentration in methanol flowing through the packed bed (in interparticle space), ϵ [–] – the bed porosity, u [m/s] – liquid interstitial velocity, D_L [m²/s] – axial dispersion coefficient, d_p [m] – sorbent particle diameter, N_{DBT} [mol/m²s] – molar flux for convective mass transfer from the liquid bulk to the sorbent grain surface, respectively.

- DBT mass balance inside the sorbent particle

$$D_i \left(\frac{\partial^2 c_{\text{DBT},p}}{\partial r^2} + \frac{2}{r} \frac{\partial c_{\text{DBT},p}}{\partial r} \right) - \rho_s (1 - \epsilon_p) \frac{\partial q_{\text{DBT}}}{\partial t} = \epsilon_p \frac{\partial c_{\text{DBT},p}}{\partial t} \quad (\text{A.2})$$

where $c_{\text{DBT},p}$ [mol/m³] is the DBT concentration in methanol present in the sorbent pore space, q_{DBT} [mol/kg] – concentrations of the adsorbed DBT, ϵ_p [–] – adsorbent pellets porosity, ρ_s [kg/m³] – density of solid adsorbent. Notice, that Eq. (A2) was derived assuming application of the pseudo-homogenous model, so D_i [m²/s] is the effective intraparticle diffusion coefficient.

According to the used approach the concentration $c_{\text{DBT}} = f(z, t)$ depends on the axial location in the adsorption column and the time, while the concentrations $c_{\text{DBT},p} = g(z, r, t)$ and $q_{\text{DBT},p} = h(z, r, t)$ depend additionally on the radial position in the sorbent grain.

The molar flux appearing in Eq. (A.1) can be expressed as follows:

$$N_{\text{DBT}} = k_f [c_{\text{DBT}} - c_{\text{DBT},p}(r = R)] = D_i \left(\frac{\partial c_{\text{DBT},p}}{\partial r} \right)_{r=R} \quad (\text{A.3})$$

where k_f [m/s] is the mass transfer coefficient. Eq. (A.3) is also formally the external boundary condition, which binds the DBT concentrations outside (c_{DBT}) and inside ($c_{\text{DBT},p}$) the sorbent particle.

The adsorption rate – while assumed to be the first order – can be expressed as:

$$\frac{dq_{\text{DBT}}}{dt} = k_{1,ad} (q_{\text{DBT},eq} - q_{\text{DBT}}) \quad (\text{A.4})$$

where $k_{1,ad}$ [1/s] is the first order adsorption rate constant. The concentration $q_{DBT,eq}$ [mol/kg] is the concentration of adsorbed DBT in equilibrium to the local DBT concentration in liquid filling the pores ($c_{DBT,p}$), while q_{DBT} is just actual and local concentration of adsorbed DBT.

The equilibrium concentration $q_{DBT,eq}$ can be expressed in terms of the DBT pore concentration $c_{DBT,p}$ according to the adsorption equilibrium equation. For Langmuir equation it reads as (Wen et al., 2010):

$$q_{DBT,eq} = \frac{q_m K_L c_{DBT,p}}{1 + K_L c_{DBT,p}} \quad (A.5)$$

The set of model equations (Eqs. A.1–A.2) can be solved taking into account Eqs. (A.3–A.5) and with the following initial conditions:

$$c_{DBT}(z, 0) = 0 \quad (A.6)$$

$$c_{DBT,p}(z, 0) = 0 \quad (A.7)$$

$$q_{DBT}(z, 0) = 0 \quad (A.8)$$

together with the following boundary conditions:

- the Danckwerts boundary conditions for the packed bed:

$$u_{c_{DBT},in} = u_{c_{DBT}} - D_L \frac{\partial c_{DBT}}{\partial z} \quad \text{at } z = 0 \text{ and at any time} \quad (A.9)$$

$$\frac{\partial c_{DBT}}{\partial z} = 0 \quad \text{at } z = L \text{ and at any time} \quad (A.10)$$

- the symmetry condition in the adsorbent grain

$$\frac{\partial c_{DBT,p}}{\partial r} = 0 \quad \text{at } r = 0 \quad (A.11)$$